2024 IEEE International Conference on Robotics and Automation (ICRA 2024)
May 13-17, 2024. Yokohama, Japan

Tendon-Driven Continuum Robot for Deep-Sea Application

Cora Maria Sourkounis[1], Tom Kwasnitschka[2] and Annika Raatz[1]

***Abstract*— The extreme conditions of the deep sea require the use of large and expensive diving robots designed to withstand the high pressure in these depths. In order to reduce the costs for sediment sampling in the deep sea and thus facilitate the explorations of rare deep-sea ecosystems, the goal of this research is to design an alternative manipulator for deep-sea suction sampling. Instead of relying on heavy hydraulic rigid manipulators that deep-sea diving robots are commonly equipped with, we introduce a new concept for a lightweight actuation system that can be used in combination with a traditional diving robot and a suction sampling system. The proposed concept consists of a series of rigid links connected by angled swivel joints. Each segment is actuated by tendons, which allows for continuous bending. The system can be adapted to various sizes of host systems, and the links and joints are printed in place, simplifying the manufacturing process.**

I. INTRODUCTION

The deep ocean, still largely uncharted, sparks increasing interest beyond the extraction of resources like oil, gas, minerals, and food. Environmental concerns, natural hazards, and its carbon cycle's role in climate change draw attention. Due to the harsh conditions caused by the combination of high pressure, low temperature, and darkness, research in these areas relies on robust, autonomous or remotely operated diving robots, which are equipped with cameras and different sampling tools. One valuable exploration method that provides us with information about the deeps sea involves sediment sampling using a suction sampler [1]. The traditional suction sampler comprises a tube operated by a hydraulic manipulator, along with sample container compartments for sediment jars. By creating a vacuum, the sediment is transported through the sampling tube into the containers [2]. The suction sampler is part of the standard equipment of an intervention-class Remotely Operated Vehicle (ROV), which is a specific type of deep-sea rated robots that is commonly used for ocean explorations in up to 6000 m depth. These systems are very expensive due to their high-tech equipment and the need for special corrosion resistant and buoyancy regulating materials. Apart from the system itself, employing these robots comes at a high cost, considering they can weigh up to 5000 kg. This necessitates the use of multiple shipping containers for both the robot and the required equipment during transportation [3].

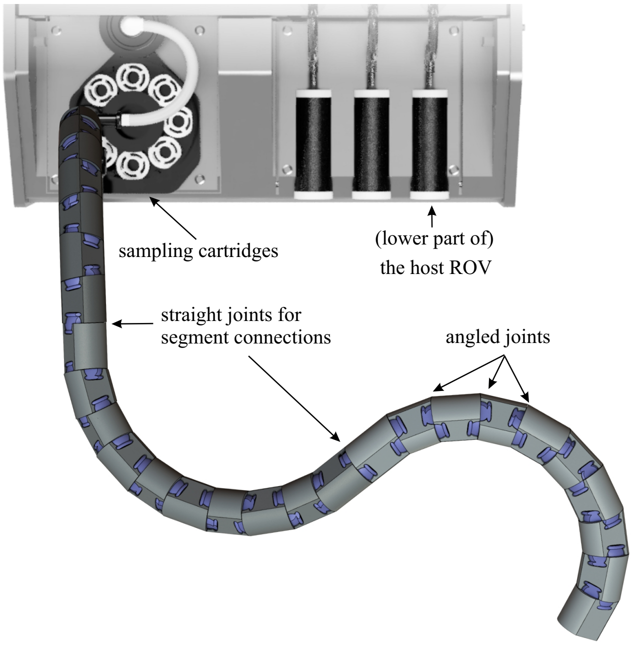

Fig. 1. The concept for improving sediment sampling in the deep sea involves the combination of an deep-sea rated ROV, which is partially depicted in the upper part of the rendering, and a novel actuation structure for the suction sampling system. The design of the affordable, scalable, and modular actuation system for the suction sampler comprises three individual segments capable of independent actuation, enabling bending through angled joints. Furthermore, at the base of each segment a straight joint connection allows for torsional motion of each segment.

To decrease the efforts for sediment sampling, a collaboration with the GEOMAR Helmholtz Centre for Ocean Research in Kiel, Germany and the Institute for Assembly Technology at the Leibniz University in Hannover, Germany was initiated. The GEOMAR regularly deploys their intervention class ROV Kiel 6000 on research expeditions into the deep sea for various sampling tasks. The Kiel 6000 is equipped with two titanium manipulators that are actuated hydraulically. These manipulators can handle various tools like chainsaws, chisels, and the above mentioned suction sampler. To cut overall costs and enhance deep-sea sediment sampling accessibility, we considered replacing or supplementing the current hydraulic titanium robot with a lightweight, scalable, and reconfigurable robotic system. This would maximize the ROV's efficiency by enabling simultaneous usage of the manipulator and the suction sampler. Alternatively, replacing the hydraulic arm could result in a reduction of the overall system's weight. The new actuation system must endure both extreme water pressure and strong underwater currents. It must withstand the deployment process, which involves

---

*Funded by the Deutsche Forschungsgemeinschaft (DFG, German Research Foundation) under grant no. 498342743.

[1] Cora Maria Sourkounis and Annika Raatz are with the Institute of Assembly Technology, Leibniz University Hannover, Germany. `sourkounis@match.uni-hannover.de`

[2] Tom Kwasnitschka is with the GEOMAR Helmholtz Centre for Ocean Research Kiel, Germany.

979-8-3503-8457-4/24/$31.00 ©2024 IEEE

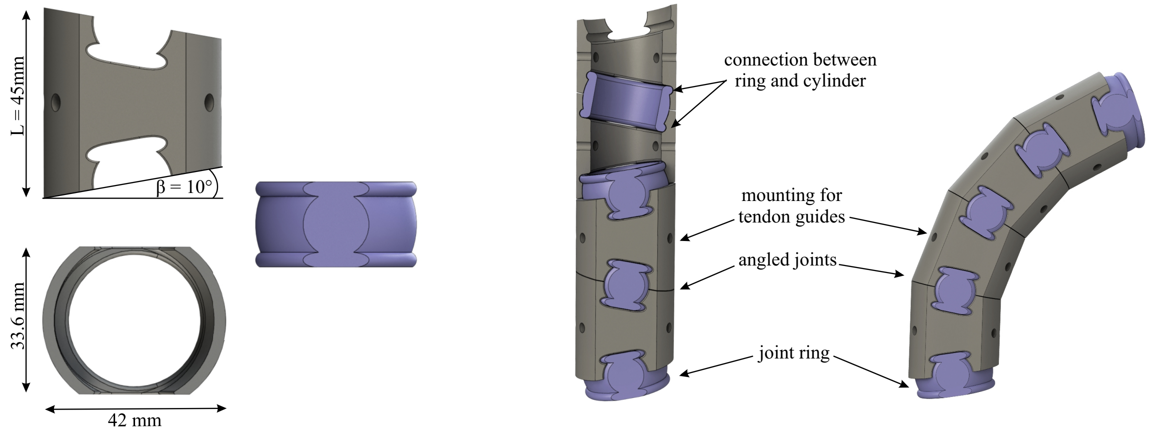

(a) Cylindrical link and joint ring

(b) Print-in-place assembly of the strucuture

Fig. 2. The bevelled cylinders are connected by swivel joints that allow cylinders to be rotated into a bent configuration. The design is intended to be 3D printed in a single piece (as shown on the right) using Fused Deposition Modeling (FDM). To print all the parts in place, cutouts were added to the sides of the structure. The renderings of the separate components in (a) serve solely to clarify the design of the joint rings and the cylindrical links. The values of L and β equal those chosen for the proof of concept. However, it is intended to adapted them to optimize the workspace of the whole system, as discussed in the modeling section.

plunging the entire ROV system into the ocean from a crane. These requirements for a lightweight, compact and deep-sea proof actuation system, sparked the idea of a continuous or snake-like system that encloses the sampling tube and thus allows for a more direct and compact actuation.

II. State of the Art

A continuous robot arm does not consist of discrete links and joints. Instead specific structures allow for continuous bending along the backbone, which proves advantageous when a compliant and flexible structure is desired. But when high forces are applied these structures are susceptible to buckling and unpredictable bending [4], which needs to be taken into account when designing a continuous deep-sea robot. Between the opposing concepts of continuously bending robots and traditional rigid manipulators, there also exist structures known as snake-like or serpentine structures. This concept defines a robot that has a very high number of joints, which results in a high dexterity [5], which already proved to be usefulness for different industrial applications such as welding, inspection tasks [6], and aircraft assembly [7]. In untethered snake robots, the big number of independent joints allows for complicated locomotion methods such as serpentine locomotion [8]. Since they were first introduced in the 1970s [9], numerous untethered robots inspired by snakes have been presented. Prominent examples for under-water snake inspired robots include the waterproof snake robot Mamba [10] and the underwater inspection robot Eelume. The Eelume robot has already undergone trials at a depth of 150 m. With developers working to enhance its pressure resistance, this robot might be used for future deep-sea exploration. However, its thruster system limits its ability to collect sediment samples [11]. Xue et al. introduced a tethered snake-like manipulator tailored for deep-sea usage, comprised of seven joints, each with two degrees of freedom. This configuration grants the snake-arm a high degree of dexterity. However, the entire arm is operated by 14 motor systems, leading to a considerable size of the actuation system [12]. To make the actuation system as compact as possible, lightweight and robust, the concept presented in this work (figure 1) is composed of numerous discrete joints that are not individually actuated, but rather in segments, enabling continuous bending over one segment. The joints are characterized by angular rotation, causing the entire structure to bend in a specific direction when they are turned. In the literature this type of joint was already introduced as a very robust option for snake robot joints [13]. However, in this study, each joint was individually actuated. Our concept, on the other hand, suggests actuating multiple joints with a single tendon, thereby aiming for a simplified and robust system. The centralized actuation unit will also serve the requirement for a pressure neutral concept for the actuation.

In the following sections the requirements and concept for the deep-sea actuation system will be described in more detail, followed by a modeling approach concerning the kinematic of the structure, which also includes the evaluation of the expected workspace of the system. Finally, the manufacturing and testing of a first proof of concept will be addressed.

III. Concept

This section outlines the initial requirements and subsequently derived concept for the actuation system of the suction sampler.

A. Requirements

The requirements for the actuation system were developed by expert users of the existing suction sampling system that is already part of the Kiel 6000 equipment of the GEOMAR research center. With regard to the current status of the research the following section will only address the

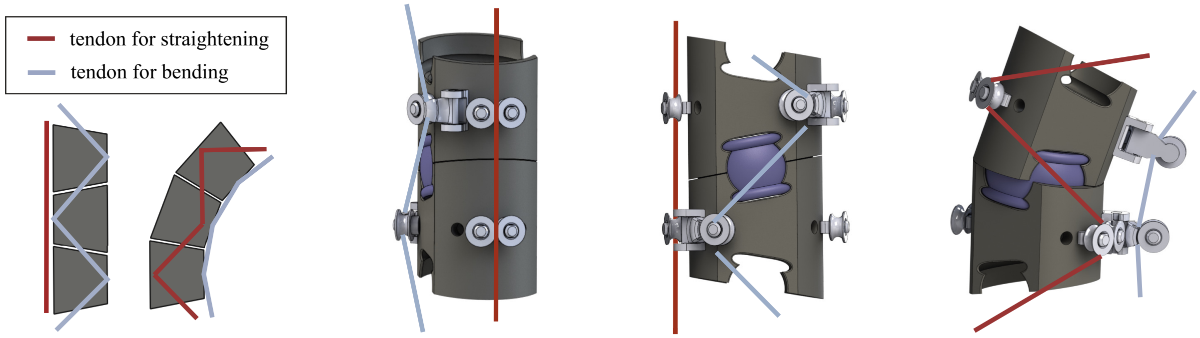

(a) Schematic illustration of the tendons

(b) Renderings of the tendon guides from different perspectives

Fig. 3. The actuation concept proposes to arrange the tendons in a way that they form a zigzag pattern, while the opposite tendon is stretched straight. To fasten the tendon on the cylinders, two different designs were used. The guides for the straightening tendons consist of two pulleys that are arranged tangentially to the cylinders' surface. For the bending tendon, a pulley was attached to a hinge that folds outwards, while the structure bends, to avoid the tendon from being pulled out of the guides.

requirements that concern the mechanical design of the system:

Most importantly, the system should operate at a depth of 6000 m, making a pressure-neutral design highly desirable. This involves choosing the materials and manufacturing with the goal of avoiding any air pockets within components. All the parts that are installed as part of the system must be adaptable in terms of dimensions, layout, and fabrication process. External components, such as motors, should be selected from a range of scalable products to ensure flexibility in fitting various sizes of host vehicles. The required modularity also involves easy access to all parts that might be at risk of breaking. The entire system must be designed to be close to neutrally buoyant, meaning no metal parts should be incorporated into the design. To avoid pollution, instead of using a traditional hydraulic system, other actuation approaches should be considered. The final version of the actuation system should match the length of the current sampling tube, which is approximately 2-3 m long. This also includes that the workspace of the suction sampler allows for sampling sediments while the host ROV hovers around 1 m above the seafloor so as to not disturb the sediments. The workspace additionally needs to be located within the field of view of the camera that is positioned at the top of the ROV. As the power is supplied via a cable ranging from the ship down to the diving robot, the whole system should be as energy efficient as possible.

The workspace that needs to be covered by the structure is defined by the field of view of the camera with which the ROV is equipped, so that the user can steer the suction sampler in the direction of the sediments. If the view and the path to the targeted sediments are blocked, the entire ROV must be repositioned. Additionaly measures for obstacle avoidance are therefore not required.

B. Links and Joints

The concept for a long tendon-driven robot consists of stacked, bevelled cylindrical links, as illustrated in figure 2. The center of the structure is hollow to allow the placement of the sampling tube. The cylinders are connected to each other by joints that only allow rotational motion around the z-axis. Due to the shape of the cylinders, the individual turning motions add up to the whole structure bending.

While connecting the cylinders with a ball-bearing could have been a straightforward solution, it would introduce metal components to the structure that are susceptible to corrosion in the saltwater environment of the deep sea. Instead, it is beneficial to manufacture the whole system out of plastic to prevent corrosion. This led to a design in which a ring instead of a ball-bearing was used to connect the cylinders. These joint rings create more friction than ball-bearings, but the print-in-place design simplifies the assembly of the whole structure.

C. Actuation

Because the actuation unit needs to be pressure neutral, it makes sense to centralize the actuation at the base of the robot. To come up with a robust actuation system, that is not affected by pressure, a tendon actuation was chosen to be combined with the mechanical structure of this robot. As a result, the cylinders cannot be actuated individually. Instead, each segment is connected by two tendons that rotate the cylinders simultaneously. In figure 3(a) the concept for the course of the tendons along the structure is illustrated.

D. Tendon guides

The main concern for the actuation of the structure were the guides for the tendons, as they cannot cause to much friction, because this would hinder the turning motion of the cylinders.

After assessing different options for the tendons, a parachute chord with a diameter of 4 mm was chosen. Other more thin tendons, like kevlar tendon or wire, showed the tendency to cut into the soft material of the structure and caused a lot of friction. To avoid friction each tendon guide

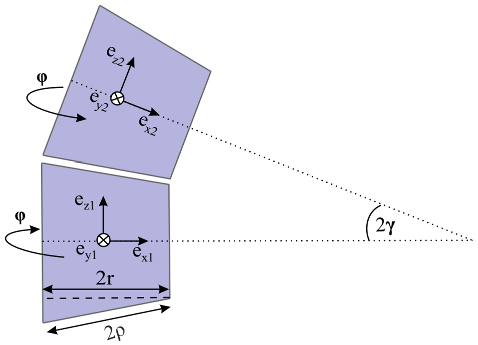

Fig. 4. The bending angle γ depends on the rotational angle of ϕ. The bending angle of a complete segment equals $N * 2\gamma$, with N representing the number of cylindrical links.

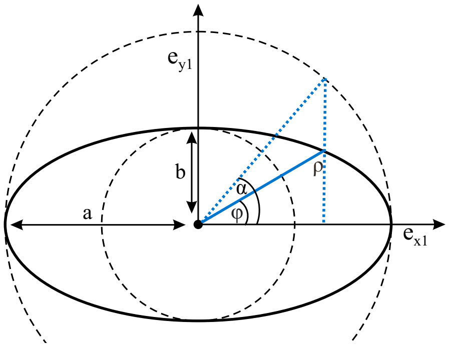

Fig. 5. The contact planes between the links have the shape of an ellipse. The defining parameters of an ellipse are the semi-major-axis a, the semi-minor-axis b and the resulting eccentricity ϵ.

was equipped with pulleys that rotate whenever the tendon is pulled.

We propose two different actuation guides: One for the straightening tendons and one for the bending tendons. The guides for the tendons, which straighten the segment, consist of pulleys that are placed tangentially on the outer surface of the cylinders. To facilitate the rotation of the cylinders, which in turn causes the structure to bend, it was found advantageous to attach the guiding pulley to a hinge that unfolds during the bending motion. This choice was made because, during bending, the forces acting on the tendon partially point away from the cylinder. Using the same guides as those employed for the straightening tendon would result in the tendon becoming trapped between the gears and thus, restricting the motion of the cylinders.

Figure 3(b) illustrates the two types of tendon guides, featuring different perspectives and configurations. While the first two images depict the straight configuration, the final image showcases the bent configuration with the hinges unfolded outward.

E. Complete System

The presented concept has the advantage that the structure is robust and requires relatively low actuation effort, as each segment is actuated by tendons. On the downside the motion of a single segment is restricted to planar bending. To create a sufficient workspace, the goal is to combine three individually actuated segments to create the actuation system for the sampling tube. For designing the complete structure, it could be beneficial to vary the length and the bending angle for the different segments by adjusting the angle β and the length of the cylinders. The bending radii should be defined in a way so that the system can be rolled up during the launching and recovery of the diving robot or in the case of extreme underwater currents. To evaluate the system's workspace in more detail, the next section provides a geometric analysis of the structure.

IV. MODELING

In this section the relation between the turning of the individual links and the resulting curvature is described. The presented approach is based on the geometry of the structure and does not include the relation between the tendon actuation and the resulting turning motion of the links.

The schematic representation of the cylindrical links can be found in figure 4. The angle ϕ represents the rotation of one cylinder around its z-axis. Thus, this value serves as the input variable for the geometrical analysis of the structure. Rotating a link by ϕ results in the link being tilted around the y-axis by the angle γ. To calculate γ, the radius r of the cylinder and ρ are inserted into the following equation:

$$\gamma = \arccos\left(\frac{r}{\rho}\right) \tag{1}$$

The variable ρ describes the radius of the ellipse depending on the rational angle ϕ. To calculate ρ, one needs to take a closer look at the geometry of the contact plane between the cylindrical links. The shape of one link is based on a cylinder that is cut at each end with an angle of β. This leads to the upper and lower plane having the shape of an ellipse. Figure 5 depicts the defining measures of an ellipse: a and b are the semi-major-axis and the semi-minor-axis respectively. To calculate the distance ρ from the turning angle ϕ, equation (2) is used, with equation (3) defining the eccentricity ϵ of the ellipse [14] [15]. To determine the semi-major-axis a equation (1) can be applied: If γ equals the maximum tilting angle of β, ρ equals a. The length of the semi-minor-axis b equals the cylinder's radius r.

$$\rho = \frac{b}{\sqrt{1-(\epsilon\cos(\phi))^2}} \tag{2}$$

$$\epsilon = \sqrt{1-\frac{a^2}{b^2}} \tag{3}$$

The coordinate transformation from one cylindrical link to the next is a combination of a rotation around the y-axis by 2γ and an offset l along the z-axis, which equals the mean length of the links.

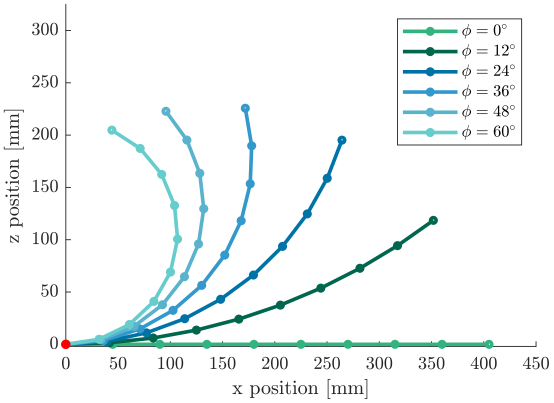

Fig. 6. This plot represents the curvature of one segment consisting of nine angular, cylindrical links in relation to the rotational angle ϕ. The values of ϕ are restricted by the design of the tendon guides and range from 0 ° to 60 °.

$$T_{yj} = \begin{pmatrix} \cos(2\gamma_j) & 0 & -\sin(2\gamma_j) & 0 \\ 0 & 1 & 0 & 0 \\ \sin(2\gamma_j) & 0 & \cos(2\gamma_j) & l \\ 0 & 0 & 0 & 1 \end{pmatrix} \tag{4}$$

$$T_y = T_{y1} * T_{y2} * ... * T_{yN} \tag{5}$$

For the description of the whole segment, the coordinate transformation matrices of each cylinder are combined. The bending angle of the whole structure adds up to $N * 2\gamma$, with N describing the number of cylinders the considered structure consists of.

In figure 6 the configuration of a segment consisting of nine cylinders depending on the turning angle ϕ is depicted. The angle ϕ ranges from $\phi_{min} = 0°$, which equals the straight configuration of the structure, and $\phi_{max} = 60°$ for the maximum bending that can be achieved. The structure of cylinders alone would allow for ϕ to be increased to up to 90°, but the rotation is limited by the positioning of the tendon guides. Rotating the cylinders further than 60° is expected to cause too much friction between the tendons and the tendon guides.

A. *Workspace*

The design of the actuation unit for the suction sampler is required to be adaptable to different host ROV and application scenarios. Using the kinematic model of the structure, the workspace of different configurations of the complete system, exemplary length of 1.5 m, was sampled. In figure 7 the assumed structure consists of three segments, which exhibit the same length and bending radius. The depicted workspace only includes configurations of different bending angles and neglects the torsional joints that connect the individual segments. It is noteworthy that the main part of the workspace is located underneath the ROV and thus does not allow the control of the suction sampling, as the camera view is restricted by the ROV's body. If the first segment is longer than the other two, while the overall length stays the same, the resulting workspace (figure 8) is more fitting for the task of suction sampling, as it is located within the camera's field of view. Additionally to the length the bending radius was adjusted by varying the angle β (figure 2).

To reduce the actuation effort it could be considered to only equip the last two segments with a torsional joint. For the first segment that is connected to the ROV, a torsional joint would not be beneficial as the suction sampling does not involve any tasks that require motion above the lower part of the ROV. Instead, a joint could be added that allows the complete structure to fold underneath the ROV in case

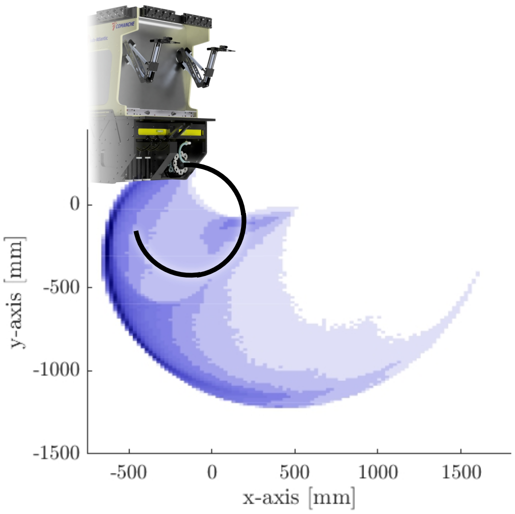

Fig. 7. When sampling the workspace while assuming the same length and bending radius for all segments. The planar workspace, which does not consider torsional motion of the individual segments, is located beneath the ROV and outside the camera's field of view. For this illustration, an exemplary length of the robot of 1.5 m was assumed.

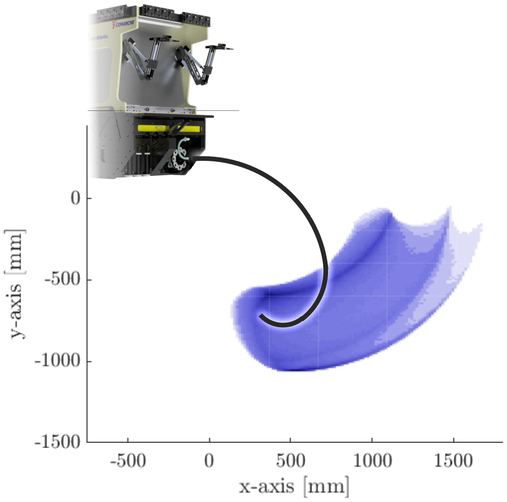

Fig. 8. Due to the longer first segment with a smaller bending radius, the workspace is located in front of the ROV which enables the user to control the sampling based on the camera view. The bending radius can be influenced by adjusting the length L and the angle β in the design of the individual cylinders.

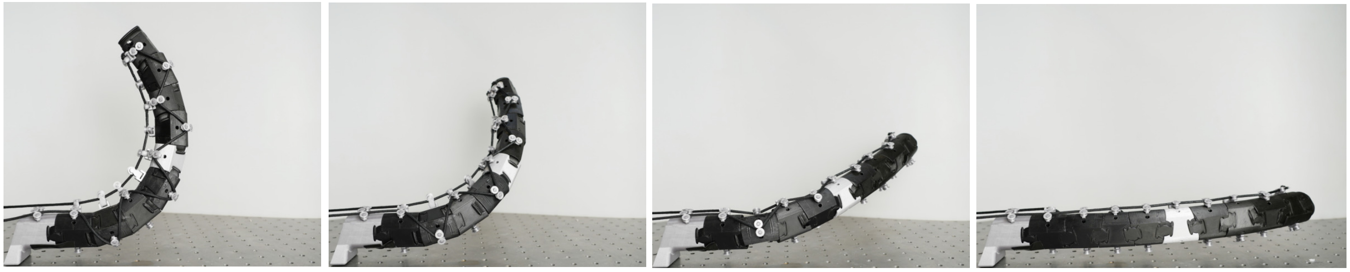

Fig. 9. The prototype was printed in two parts. The light grey link was printed in two parts to connected the sections of the prototype. The structure was actuated with a preliminary actuation system that allowed the manual control of the motors rotating the cable winch. The sequence of images demonstrates that the behavior of the structure deviates from the predicted behavior of the kinematic model. This is primarily due to the significant friction between the links. Nevertheless, the structure proved to be robust and functional.

of extreme water currents and during the deployment of the robot.

V. PROTOTYPE

The prototype was manufactured from PLA using a Prusa MKS3+, which allowed for quick and cheap prototyping. The structure is designed in a way that the cylinders and joints for one segment can be printed in one piece. But because of the size of the printers build plate the segment had to be split in half. To assemble the structure, one link was cut in half for printing. The Fused Depositing Modeling (FDM) technology, the printer uses, creates a very uneven surface, which increases the friction between the moving parts. Still, this manufacturing method was sufficiently precise to print the joints of the structure in place. To improve the manufacturing accuracy and create smoother surfaces a more elaborate manufacturing method could be considered in the future. The tendon guides have to be printed as separate parts and are attached to the main structure.

In order to test the concept, one segment consisting of nine angled cylinders and one straight joint was manufactured.

A. Discussion

To evaluate the motion of the robot, a manually controlled actuation unit consisting of two cable winches and two stepper motors was assembled. It allowed the user to shorten and elongate the two tendons individually or simultaneously. To ensure that the structure remains upright, at least one tendon must always be under tension, which is a challenge when adjusting the tendon length manually.

The sequence of images in figure 9 shows the motion of the structure from straight to fully bent. Against initial expectations gathered from the modeling, the individual cylinders do not evenly turn at the same time. Instead, the lower cylinders turn first and the motion proceeds to the tip of the segment. This caused the structure to tilt out of the xz-plane during the bending motion. The last cylinders also do not turn fully, which causes inconsistent bending over the course of the structure. One reason for this behaviour is the high friction between the links and joints and the friction between the tendon guides and the tendons themselves. To improve the bending and the accuracy of the kinematic model, the friction in the structure could be reduced by choosing a more precise manufacturing method. Additionally, the model should be developed further and the impact the friction has on the motion should be considered.

To further validate the concept, underwater tests will be carried out in the next steps, which require the attachment of a protective skin to ensure that the tendons are not exposed to environmental influences.

Despite the addressed challenges, the design concept has demonstrated sufficient curvature and robustness. When equipped with a more elaborate actuation unit, it is anticipated to have the capacity to withstand a substantial payload.

VI. CONCLUSION AND FUTURE WORK

In this paper a concept for a tendon actuated deep-sea suction sampler was presented. The concept includes the design of the mechanical structure as well as the tendon actuation. The design was focused on the structure being lightweight and robust. Additionally, it is easy to assemble as most parts can be printed in place. The kinematic model of the structure was presented and, finally, a proof of concept was manufactured to evaluate the viability of the concept and to evaluate the kinematic model that was implemented based on the geometry of the structure. As the concept proved to be functional, future work will include the implementation of an actuation system and a matching kinematic analysis for the actuation. Furthermore, a more precise manufacturing method should be considered to decrease the friction between the links and joints. While improving the design to reduce the friction within the joints, it should also be considered to include the impact of friction in the modeling of the robot's behaviour.

REFERENCES

[1] H. Huneke and T. Mulder. *Deep-Sea Sediments*. Elsevier, 2011. ISBN: 9780444530004.

[2] Keith Shepherd and S Kim Juniper. "ROPOS: Creating a scientific tool from an industrial ROV". In: *Article in Marine Technology Society Journal* 31 (3 1997), pp. 48–54.

[3] Romano Capocci et al. “Inspection-class remotely operated vehicles-a review”. In: *Journal of Marine Science and Engineering* 5 (1 Mar. 2017). ISSN: 20771312. DOI: `10.3390/jmse5010013`.

[4] Ian D. Walker et al. “Challenges in creating long continuum robots”. In: Institute of Electrical and Electronics Engineers Inc., Sept. 2016, pp. 339–344. ISBN: 9781509018666. DOI: `10.1109/MMAR.2016.7575158`.

[5] G. Robinson and J.B.C. Davies. “Continuum robots - a state of the art”. In: vol. 4. IEEE, 1999, pp. 2849–2854. ISBN: 0-7803-5180-0. DOI: `10.1109/ROBOT.1999.774029`.

[6] Richard Bloss. “Snake-like robots ”reach” into many types of applications”. In: *Industrial Robot* 39 (5 2012), pp. 436–440. ISSN: 0143991X. DOI: `10.1108/01439911211249724`.

[7] Rob Buckingham et al. “Snake-Arm Robots: A New Approach to Aircraft Assembly”. In: Sept. 2007. DOI: `10.4271/2007-01-3870`.

[8] Pål Liljebäck et al. *Snake Robots*. Springer London, 2013. ISBN: 978-1-4471-2995-0. DOI: `10.1007/978-1-4471-2996-7`.

[9] Shigeo Hirose, Peter Cave, and Charles Goulden. *Biologically Inspired Robots: Serpentile Locomotors and Manipulators*. USA: Oxford University Press, Inc., 1993. ISBN: 0198562616.

[10] Pal Liljeback et al. “Mamba - A waterproof snake robot with tactile sensing”. In: Institute of Electrical and Electronics Engineers Inc., Oct. 2014, pp. 294–301. ISBN: 9781479969340. DOI: `10.1109/IROS.2014.6942575`.

[11] Pal Liljeback and Richard Mills. “Eelume: A flexible and subsea resident IMR vehicle”. In: IEEE, June 2017, pp. 1–4. ISBN: 978-1-5090-5278-3. DOI: `10.1109/OCEANSE.2017.8084826`.

[12] Fufeng Xue and Zhimin Fan. “Kinematic control of a cable-driven snake-like manipulator for deep-water based on fuzzy PID controller”. In: *Proceedings of the Institution of Mechanical Engineers. Part I: Journal of Systems and Control Engineering* 236 (5 May 2022), pp. 989–998. ISSN: 20413041. DOI: `10.1177/09596518211064794`.

[13] Elie Shammas et al. “New Joint Design for Three-dimensional Hyper Redundant Robots”. In: vol. 4. 2003, pp. 3594–3599. DOI: `10.1109/iros.2003.1249713`.

[14] W. Hackbusch, H. R. Schwarz, and E. Zeidler. *Teubner-Taschenbuch der Mathematik*. Vieweg+Teubner Verlag, 2003. DOI: `10.1007/978-3-322-96781-7`.

[15] J. Dennis Lawrence. *Catalog of Special Plane Curves*. Dover Publications, 1972. ISBN: 9780486602882.